

ORIGINAL ARTICLE

MORPHOLOGICAL FEATURES OF TUBULAR BONES REPARATIVE REGENERATION UNDER THE INFLUENCE OF ANTITUMOR CHEMOTHERAPEUTICS

DOI: 10.36740/WLek202203102

Tatiana V. Riabenko, Oleksii V. Korenkov, Serhii M. Dmytruk, Olha S. Yarmolenko, Alina A. Ponurko, Mykolay S. Pernakov, Viktoriia I. Gula
SUMY STATE UNIVERSITY, SUMY, UKRAINE

ABSTRACT

The aim: Determination of morphological features of reparative regeneration of diaphysis defect of long tubular bones under the influence of antitumor chemotherapeutics in a model experiment.

Materials and methods: 96 white nonlinear rats after application of the perforated defect of the femur were administered the appropriate antitumor drug (doxorubicin, 5-fluorouracil, methotrexate) three times with an interval of 21 days. Morphological features of bone tissue formation and remodeling in the regenerate area were studied using histological and morphometric methods.

Results: The inhibitory effect of antitumor chemotherapeutics on the formation of regenerate, expressed by slowing down the process of bone tissue differentiation was found. This is confirmed by a decrease in the area of reticulofibrous and lamellar bone tissue, chaotic arrangement and narrowing of bone trabeculae with uneven color, slow formation of bonding lines between the maternal bone and the regenerate.

Conclusions: The revealed morphological features of reparative regeneration of the diaphysis defect of long tubular bones under the influence of antitumor chemotherapeutics doxorubicin, 5-fluorouracil and methotrexate in a model experiment indicate a slowing of reparative regeneration processes at all stages of recovery after injury.

KEY WORDS: reparative regeneration, bone, antitumor chemotherapeutics

Wiad Lek. 2022;75(3):570-576

INTRODUCTION

The homeostatic mechanism of reparative regeneration includes the interaction of a complex of factors (osteogenic and immunocompetent cells migration, growth factors and chemotactic mediators production, an adequate vascular meshwork formation, etc.), which form the necessary proregenerative microenvironment. [1-3].

Understanding the morphological changes forming the basis of each stage of reparative bone regeneration will allow us to develop effective strategies aimed at optimizing the conditions of regeneration, activating various sources of regenerative cells, reducing the impact of processes that slow regeneration, and, ultimately, obtaining the predicted growth of bone tissue to eliminate its deficiency caused by pathological exposure [4-6].

One of the most current issues of modern regenerative medicine is solving the problem of the negative impact of chemotherapeutics used to treat cancer, often over a long period of time. With the development of cancer in the body there are disorders of bone metabolism manifested by the development of osteoporosis and bone metastasis. In particular, bone is the most common site of metastasis in patients with breast or prostate cancer. [7-10]. By colonizing bone, tumor cells interact with different cell types (osteoblasts, osteoclasts, osteocytes, fibroblasts, immune cells), form the so-called «vicious circle» in the locus of invasion, based on the ability of metastatic cells

to coax osteoclasts and osteoblasts, which further stimulate the growth of cancer cells (the concept of premetastatic niche). To date, the most characterized are the effects of VEGF (Vascular Endothelial Growth Factor) and disturbances in the system of RANKL/RANK/OPG (Receptor Activator of Nuclear Factor- κ B Ligand Osteoprotegerin) [11-13].

According to a number of retrospective studies, antitumor chemotherapy, which begins immediately after diagnosis and is prescribed for a long time, is usually associated with the loss of bone mineral density and increased risk of fractures. [14,15].

Therefore, study of bone regeneration under the influence of chemotherapeutics is current in terms of understanding the structural basis of pathophysiological processes that develop in bone under such conditions. They will provide an opportunity to develop a system of measures to reduce the negative impact of antitumor chemotherapy on the bone microenvironment, which in turn will optimize the regenerative potential of bone and solve the problem of osteoporosis that accompanies cancer.

THE AIM

The aim of the study was to investigate the morphological features of reparative regeneration of the long tubular bones diaphyses defect under the influence of antitumor chemotherapeutics in a model experiment

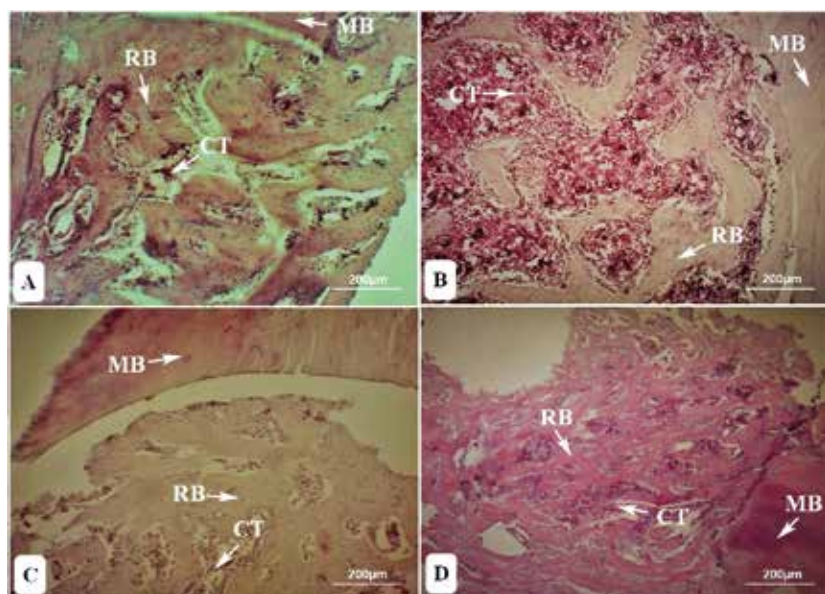


Fig. 1. Histological section of rat femur regenerate on the 15th day after the perforated defect application: A – control group, B – animals receiving doxorubicin, C – animals receiving 5-fluorouracil, D – animals receiving methotrexate. CT – connective tissue, RB – reticulofibrous bone tissue, MB – maternal bone (100x)

MATERIALS AND METHODS

The research was carried out on 96 white nonlinear male rats aged 7 months at the start of the experiment (the mean body weight was 220.0 ± 10.0 g). The animals were kept in normal vivarium conditions on a standard diet and drinking regime. The study was performed in compliance with the requirements of biological ethics in accordance with the European Convention for the Protection of Vertebrate Animals Used for Experimental and Other Purposes (Strasbourg, 1985) and the principles of research defined by the Commission on Bioethics in Experimental and Clinical Research of Sumy State University Medical Institute.

Experimental animals were divided into control (group 1, $n = 24$) and experimental (group 2, $n = 72$) groups by random sampling. In a sterile operating room, under ketamine anesthesia (50 mg/kg), all animals underwent a perforated defect in the middle third of the femoral diaphysis 2 mm in diameter, and depth to the medullary cavity using a spherical dental drill cutter under cooling. Experimental animals, in turn, were subdivided into 3 groups by random sampling. Immediately after injury, the animals of group 2.1 ($n = 24$) were injected intraperitoneally with the pharmaceutical drug doxorubicin at a dose of 60 mg/m², pre-diluted in 1.5 ml of saline, the animals of group 2.2 ($n = 24$) – with 5-fluorouracil at a dose of 600 mg/m² in 1.0 ml of saline, and the animals of group 2.3 ($n = 24$) – with methotrexate at a dose of 40 mg/m² in 1.0 ml of saline. Re-administration of appropriate chemotherapeutics was performed in the same doses on the 21st and 42nd day after injury. Animals in the control group were injected intraperitoneally with a similar volume of saline according to the same scheme.

On days 15, 30, 45, and 60 after injury, animals were removed from the experiment by decapitation under ketamine anesthesia. The traumatized femur diaphyses were fixed in 10% formalin solution on phosphate buffer for 24 hours. Decalcification was performed in 5% nitric acid solution for 14 days (solution was replaced daily) at room temperature. The completeness of decalcification was determined by a needle test. Then the test material was washed with running water followed

by dehydration in alcohol solutions of increasing concentration. After dehydration, the samples were embedded in paraffin. Histological sections of 6–10 µm thickness were made with a rotary ultramicrotome Shandon Finesse 325 (Thermo Scientific, USA). Preparations were stained with hematoxylin and eosin. Histological analysis was performed using a microscope «Carl Zeiss Primo Star» (Germany) at magnifications of x100 and x200. Photodetection was done by the digital camera «AxioCfm ERc 5s» (Carl Zeiss, Germany) with the image output «ZEN 2» (blue edition) (Carl Zeiss, Germany).

For morphometric analysis we applied a computer program for processing histological images «Digimizer», namely such tools as a microgrid and a micro ruler. The following parameters were measured in the area of rats' femur defect: the area of connective tissue (Ac), the area of reticulofibrous bone tissue (Arb), and the area of lamellar bone tissue (Alb).

Statistical analysis of the obtained data was performed using the software package Statistica v.10 («StatSoft Inc.», USA). We calculated the mean value (M) and standard deviation (SD) by descriptive analysis of each sample. After checking the distribution of data for normality, we used Student's t-test to assess differences between independent samples. A probability level (p-value) of less than 0.05 was considered to be statistically significant.

RESULTS

15TH DAY OF THE EXPERIMENT

In the control bone regenerate, the Arb in the defect is $43.83 \pm 5.88\%$, the Ac – is $56.17 \pm 3.87\%$. The reticulofibrous bone tissue is represented by trabeculae, which form large-looped mesh structures with numerous primary osteoblasts and osteocytes. Newly formed trabeculae are stained unevenly and less intensely compared to the maternal bone, indicating the beginning of ossification. The intertrabecular space is filled with connective tissue with fibroblasts, collagen fibers, and vessels. In the maternal bone, alongside the

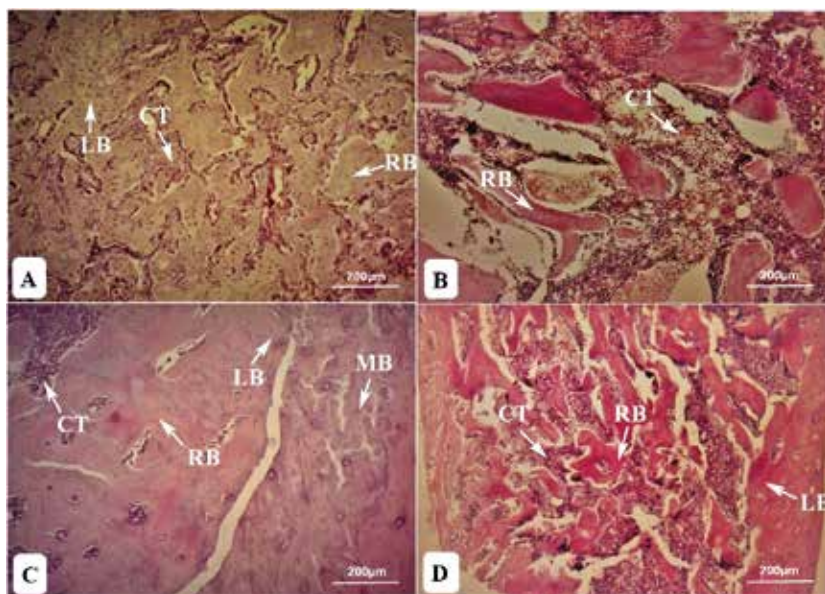


Fig. 2. Histological section of rat femur regenerate on the 30th day after the performed defect application: A – control group, B – animals receiving doxorubicin, C – animals receiving 5-fluorouracil, D – animals receiving methotrexate. CT – connective tissue, RB – reticulofibrous bone tissue, LB – lamellar bone tissue, MB – maternal bone (100x).

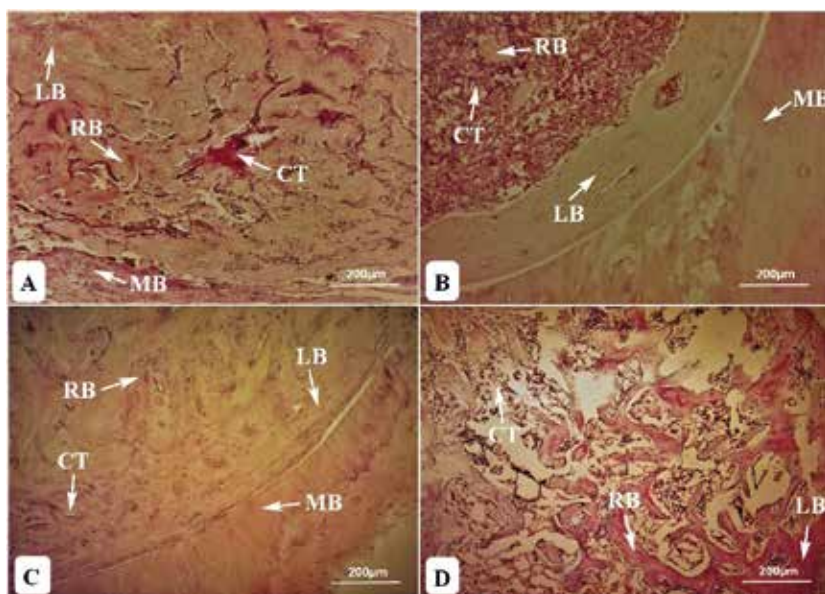


Fig. 3. Histological section of rat femur regenerate on the 45th day after the performed defect application: A – control group, B – animals receiving doxorubicin, C – animals receiving 5-fluorouracil, D – animals receiving methotrexate. CT – connective tissue, RB – reticulofibrous bone tissue, LB – lamellar bone tissue, MB – maternal bone (hematoxylin and eosin, 100x).

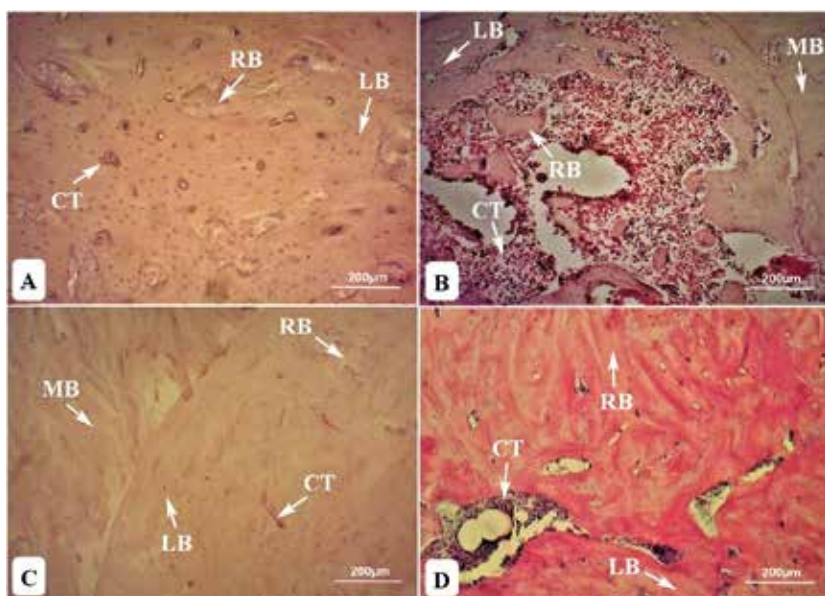


Fig. 4. Histological section of rat femur regenerate on the 60th day after the performed defect application: A – control group, B – animals receiving doxorubicin, C – animals receiving 5-fluorouracil, D – animals receiving methotrexate. CT – connective tissue, RB – reticulofibrous bone tissue, LB – lamellar bone tissue, MB – maternal bone (100x).

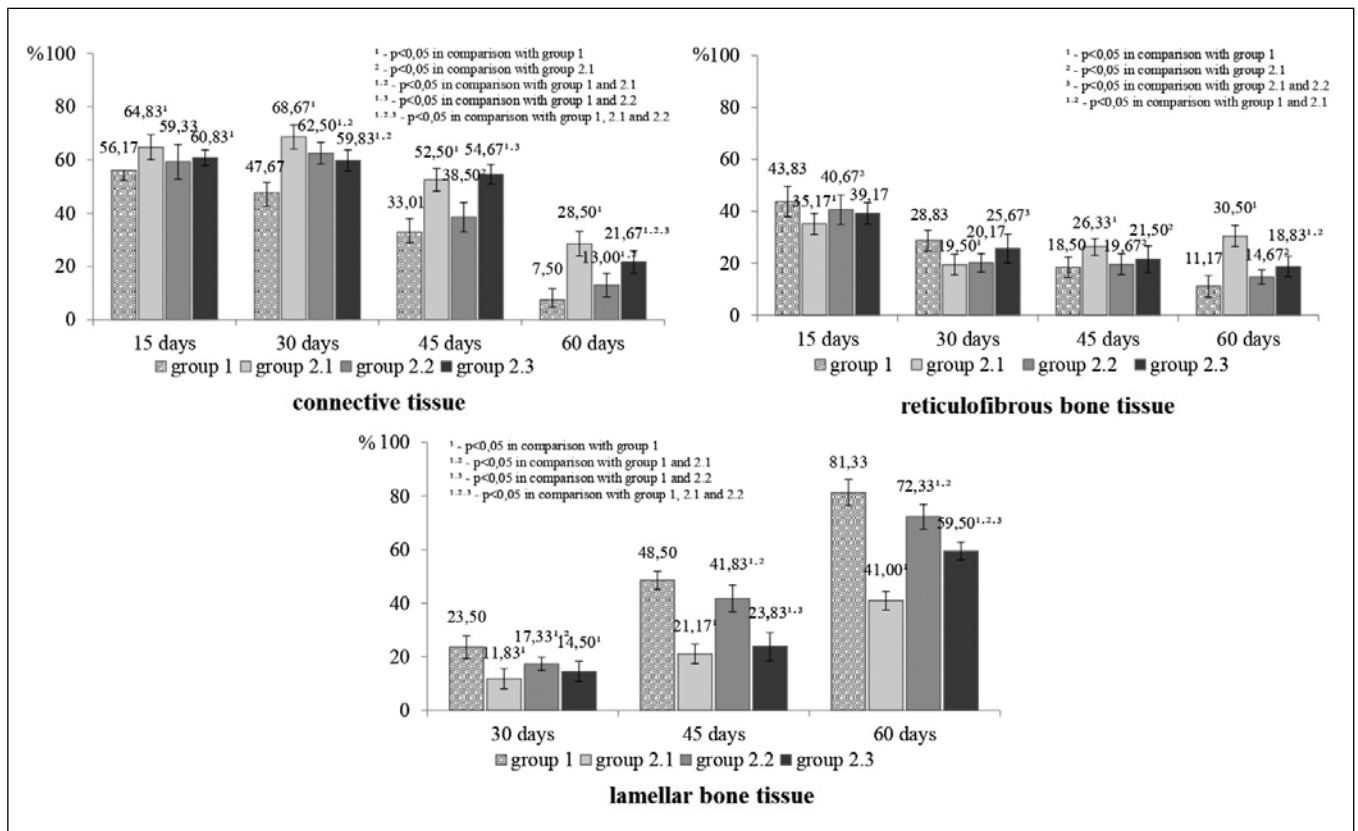


Fig. 5. Distribution of connective and bone tissue areas in bone regenerate of control and experimental groups during the experiment.

preserved cells, single empty osteocyte lacunae are located. The edges of the maternal bone are marked by signs of resorption. The boundary between the edges of the defect and the regenerate is clearly visualized (Fig. 1A).

In the group 2.1 bone regenerate the Arb is less by 19.75% ($p = 0.01$), and the Ac, on the contrary, is greater by 15.41% ($p = 0.006$) compared with the bone regenerate of control group. In the defect cavity, bone tissue is represented by bone trabeculae and contains primary osteoblasts, osteocytes, and osteogenic cells. The connective tissue with areas of osteogenesis is present in the intertrabecular spaces (Fig. 1B).

In the group 2.2, reticulofibrous bone tissue and connective tissue occupy $40.67 \pm 3.93\%$ and $59.33 \pm 6.50\%$ of the total defect area, respectively. The differences between these indicators in the control group and the group 2.2 are insignificant, but their probable direction, namely, a decrease in the Arb by 7.21% ($p = 0.29$) and an increase in Ac by 5.62% ($p = 0.33$), is similar to that of the group 2.1 (Fig. 1C).

In the regenerate of group 2.3, in comparison with the control group, there is an increase in the Ac by 8.29% ($p = 0.04$) ($60.83 \pm 2.99\%$). The indicator of the Arb ($39.17 \pm 4.17\%$) does not significantly differ from the same indicator in control animals, but the probable direction of changes in group 2.3 is towards a decrease in the indicator by 10.63% ($p = 0.14$). The regenerate is represented by small-looped trabeculae mainly. The intertrabecular space is filled with connective tissue and bone marrow (Fig. 1D).

30TH DAY OF THE EXPERIMENT

In the control group the formation of complete bone regenerate is observed in the area of the defect. The regenerate is represented by lamellar and reticulofibrous bone tissues with a total area of $52.33 \pm 4.15\%$. The basic area of the defect is formed by a small-looped mesh of trabeculae with numerous osteocytes. The coloring of trabeculae is more uniform and it approaches to the maternal bone by intensity. It indicates the normalization of osteoid ossification. The cortical plate of the regenerate is represented by lamellar bone tissue fused with the edges of the defect. In the intertrabecular spaces there are preserved areas of connective tissue with a total area of $47.67 \pm 5.05\%$, which is 15.13% ($p = 0.008$) less than in the control group on the 15th day of the experiment, as well as blood vessels and bone marrow. The formation of intensely colored bone plates around blood vessels is detected. The described changes indicate the beginning of the restructuring of reticulofibrous bone tissue into lamellar (Fig. 2A).

In the group 2.1 the main part of the newly formed regenerate is connective tissue ($68.67 \pm 4.46\%$), which is 41.95% ($p < 0.0001$) more than in the control group regenerate. Bone tissue occupies $31.33 \pm 2.1\%$ of the regenerate area. This is 40.12% ($p < 0.001$) less than in the control group regenerate ($52.33 \pm 4.11\%$). It is represented mainly by reticulofibrous type with an area of $19.5 \pm 3.99\%$, in the form of single, unrelated trabeculae. The intertrabecular spaces of reticulofibrous bone tissue have the form of wide channels filled with red bone marrow with pronounced vascularization. Mainly on the regenerate periphery, around the blood vessels, there

is the formation of concentrically arranged and intensely colored bone plates. The formation of lamellar tissue is also slowed, its area is $11.83 \pm 3.71\%$, which is 49.65% ($p = 0.003$) less than in the control group. A small number of osteoblasts are located on the trabeculae surface (Fig. 2B).

In the group 2.2, the regenerate consists of 62.50% of connective tissue and 37.50% of bone tissue. The Ac is greater by 31.10% ($p = 0.0002$) than in the control group, while the area of newly formed bone tissue is correspondingly less by 39.55% ($p = 0.007$). Bone tissue is represented mainly by reticulofibrous type ($20.17 \pm 3.19\%$) and its area does not differ significantly from the same in the control group. Lamellar bone tissue occupies $17.33 \pm 2.50\%$. On the 30th day of the experiment the cortical layer between the maternal bone and the regenerate is not yet formed and has signs of remodelling. There is a free space between the regenerate and the edge of the maternal bone (Fig 2C).

In the group 2.3 regenerate, bone tissue is represented mainly by reticulofibrous type ($25.67 \pm 4.13\%$) in the form of a small-looped trabecular mesh with osteocytes. Vascular canals and structures similar to primary osteons ($14.5 \pm 3.83\%$) are formed mainly along the edges of the defect. Connective tissue occupies $59.83 \pm 4.02\%$ of the regenerate area, which is 25.50% ($p = 0.0009$) more than in the control group regenerate (Fig. 2D).

45TH DAY OF THE EXPERIMENT

In the regenerate area of the control group, the process of bone remodeling is marked by a further increase in the area of bone tissue, which averages $67.00 \pm 4.50\%$. The newly formed bone tissue is represented mainly by the lamellar type ($48.50 \pm 3.39\%$). In the central part of the defect is a small area of the connective tissue, where the collagen fibers ordering and their transformation into osteoid trabeculae is being observed (Fig. 3A).

In the group 2.1, most of regenerate is represented by connective tissue with bone marrow ($52.40 \pm 4.23\%$). At the edges of the defect there is a bone tissue with an area of $47.50 \pm 3.63\%$, main represented mainly by reticulofibrous type. However, in this locus, there is a narrowing of the space between the regenerate and the maternal bone compared to the previous term of the experiment. (Fig. 3B).

Among all components of the group 2.2 regenerate the newly formed bone tissue prevails ($61.50 \pm 4.56\%$). It is represented mainly by lamellar tissue with osteons of varying degrees of maturity. Connective tissue occupies $38.50 \pm 5.47\%$ of the regenerate. This indicator is not significantly differ from that in the control animals, but the probable tendency to delay the process of bone formation is noticeable, because the connective tissue occupies 16.66% ($p = 0.08$) more area than in the control group. In some places, there is a formation of junctions between the regenerate and the maternal bone, but it is less pronounced than in the control group (Fig. 3C).

In the group 2.3, the regenerate is represented mainly by small-looped trabeculae with an inhomogeneously colored matrix. Most trabeculae are thin, with cracks and

fissures. Bone trabeculae are arranged chaotically without matching the load lines. A small number of osteoblasts are found on the outer surface of the trabeculae and cavity walls. The intertrabecular spaces are dilated and contain connective tissue, the Ac is $54.67 \pm 3.61\%$. Blood vessels and red bone marrow are also visible in the intertrabecular spaces (Fig. 3D).

60TH DAY OF THE EXPERIMENT

In the control group, the vast majority of the defect area is represented by lamellar bone tissue (Albis $81.33 \pm 4.17\%$), with osteons of varying degrees of maturity. There are many blood vessels around which concentrically located osteons are formed. This indicates a high activity of angiogenesis in the regenerate area, which is a necessary condition for its further adequate restructuring in the area of the applied defect (Fig. 4A).

In the group 2.1, compared with the control one, the Ac ($28.50 \pm 4.64\%$) increases by 21.00% ($p < 0.0001$) and bone area ($71.50 \pm 4.52\%$) is less by 21.00% ($p < 0.0001$). The lamellar bone tissue is located mainly on the periphery of the defect. There is a narrowing of the space between the regenerate and the maternal bone with a small number of junctions (Fig. 4B).

In the group 2.2, the main part of the regenerate is formed by lamellar bone tissue ($72.33 \pm 4.63\%$). It is 11.06% ($p = 0.008$) less than the same control indicator. There is an active process of junctions formation between the maternal bone and the defect (Fig. 4C).

In the group 2.3, the regenerate consists of connective tissue (Ac is $21.67 \pm 4.27\%$). Bone tissue in the defect area is $78.33 \pm 3.54\%$, which is 15.31% less than in the control group. The lamellar tissue fills $59.50 \pm 3.27\%$ of the regenerate area, which is 26.84% ($p < 0.0001$) less than the control indicator (Fig. 4D).

Quantitative data on the area of connective and bone tissues distribution in the regenerate in the dynamics of the experiment is presented in Fig. 5.

DISCUSSION

The current study was aimed at determining the morphological features of bone tissue reparative regeneration under the influence of the most widely used antitumor chemotherapeutics.

The vast majority of patients with cancer should take long courses of antitumor chemotherapy. This is one of the causes of bone mass loss due to impaired bone microarchitecture, which reduces skeletal strength and increases the risk of fractures, usually of the spine (compression fractures of the vertebrae), thighs and wrists. Further reparative regeneration of bone tissue also occurs under the influence of chemotherapeutic drugs, which, of course, affect the speed and quality of regenerative processes [16].

Under physiological conditions, reparative regeneration occurs according to the stages of the bone defect healing, namely through the newly formed reticulofibrous bone

tissue, which over time occupies an increasing defect area and undergoes appropriate remodeling with subsequent formation of lamellar bone tissue and its fusion with the maternal bone. [17-19].

The use of antitumor chemotherapeutics, in particular doxorubicin, 5-fluorouracil and methotrexate, in a model experiment leads to a slowing of reparative regeneration, which is manifested by a delay in the regenerate formation due to slowing tissue differentiation. This is confirmed by a slow decrease in the Ac and Ar along with a relatively slow increase in the Al in the defect. Changes in the microarchitecture of the defect area under the influence of these antitumor chemotherapeutics are characterized by chaotic location of bone trabeculae, which are relatively smaller, by the presence of free space between the maternal bone and regenerate, by low rates of bonding lines between them. The most pronounced delay in the bone regenerate remodeling was observed in the use of doxorubicin and methotrexate, while 5-fluorouracil showed less inhibitory effect on these processes.

A significant inhibitory effect of doxorubicin was also found in a model experiment on young mice conducted by L. Straszowski et al. In particular, it was found that doxorubicin adversely affects the longitudinal growth of bone, inhibits differentiation and reduces the volume of both spongy and cortical bone tissue, which ultimately leads to increased bone fragility [20].

According to studies by T. Rana et al, doxorubicin increases the circulating level of Transforming Growth Factor- β (TGF β) in mice in an experiment that induces osteoclast-mediated resorption and inhibits osteoblast differentiation. This promotes the development of osteolytic bone damage and slows the reparative regeneration in bone tissue [21].

Our results are in good agreement with the data obtained by H. Fonseca et al. in an experiment on Wistar rats. The authors noted the negative impact of doxorubicin on the radial growth of the femur, the differentiation of bone tissue, its microarchitecture and mechanical properties [22].

The inhibitory effect of 5-fluorouracil on the reparative bone regeneration noted in our study correlates well with the effect of this drug described by J. Quach et al. Based on histomorphometric analysis of mouse bones, these researchers found that bone mass loss associated with using 5-fluorouracil, was caused by the inability of osteoblasts to form sufficient bone tissue mass to compensate for the increased osteoclastic bone resorption (ie, the inadequacy of the balance between bone formation and resorption). According to the authors, this is due to a change in the ratio in the system RANKL / RANK / OPG [23]. The decrease in bone tissue mineralization potential under the influence of 5-fluorouracil, despite the lack of changes in osteoblasts density on the surface of the trabecular bone was also noted in the works of C. Fan et al., K. Georgiou et al. and R. McKinnon et al. As a reason, the authors noted a decrease in the osteoblast activity, confirmed by low levels of bone alkaline phosphatase in the experimental rat serum [24].

The negative impact of methotrexate is also confirmed by the results of an experimental study by F. Robin et al., which found an increase in apoptotic osteocytes in the juvenile rat tibial metaphysis during the methotrexate chemotherapy [25]. According to K. Georgiou et al., the methotrexate causes changes in osteogenic, hematopoietic, osteoclastogenic and adipogenic bone marrow differentiation associated with impaired Wnt / β -catenin signaling. This leads to bone marrow obesity, activation of osteoclast differentiation and an increase in their number [26]. The inactivation of β -catenin in osteoblasts does not affect their activity, but causes increased osteoclastogenesis due to insufficient osteoprotegerin production. As a result, increased bone resorption causes a decrease in bone tissue mass and slows the regeneration [27].

A corresponding contribution to the development of the pathological process associated with a decrease in bone mineral density is made by increased production of proinflammatory cytokines IL-1 and IL-6 by monocytes and activation of nuclear factor kappa B (NF- κ B) under long-term methotrexate therapy [28].

CONCLUSIONS

The use of antitumor chemotherapeutics doxorubicin, 5-fluorouracil, and methotrexate in a model experiment leads to a slowdown of the long tubular bones reparative regeneration at all stages of healing of traumatic injury, expressed in a decrease in the rate of tissue differentiation in the regenerate area. The inhibitory impact of doxorubicin and methotrexate are relatively more pronounced than that of 5-fluorouracil.

REFERENCES

1. Bragdon B.C., Bahney C.S. Origin of Reparative Stem Cells in Fracture Healing. *Curr Osteoporos Rep.* 2018;16(4):490-503. doi:10.1007/s11914-018-0458-4.
2. Kanczler J.M., Wells J.A., Gibbs D.M.R. et al. Bone tissue engineering and bone regeneration. *Principles of Tissue Engineering.* 2020. doi: 10.1016/B978-0-12-818422-6.00052-6.
3. Zupan J., Tang D., Oreffo R.O.C. et al. Bone-Marrow-Derived Mesenchymal Stromal Cells: From Basic Biology to Applications in Bone Tissue Engineering and Bone Regeneration. *Cell Engineering and Regeneration, Reference Series in Biomedical Engineering.* 2020. doi: 10.1007/978-3-319-08831-0_7.
4. Oryan A., Alidadi S., Moshiri A., Maffuli N. Bone regenerative medicine: classic options, novel strategies and future directions. *J Ortho Surg Res.* 2014;9(1):18. doi: 10.1186/1749-799X-9-18.
5. Taraballi F., Bauza G., McCulloch P. et al. Concise Review: Biomimetic Functionalization of Biomaterials to Stimulate the Endogenous Healing Process of Cartilage and Bone Tissue. *Stem Cells Translational Medicine.* 2017;6:2186-2196. doi: 10.1002/sctm.17-0181.
6. Simkin J., Seifert A.W. Concise Review: Translating Regenerative Biology into Clinically Relevant Therapies: Are We on the Right Path? *Stem Cells Translational Medicine.* 2018;7:220-231. doi: 10.1002/sctm.17-0213.
7. Logosha A.I., Slisarenko A.V., Ogiyenko M.H. et al. Reparativnyy osteogenez trubchatykh kostey v usloviyakh narusheniya vodno-solevogo [Reparative osteogenesis of tubular bones in the conditions of violation of water-salt exchange]. *Georgian medical news.* 2013;10(223):80-86. (In Ukrainian).

8. Coleman R., Body J.J., Aapro M. et al. Bone health in cancer patients: ESMO clinical practice guidelines. *Ann Oncol.* 2014;25:124.
9. Gül G., Sendur M.A.N., Aksoy S. et al. A comprehensive review of denosumab for bone metastasis in patients with solid tumors. *Curr Med Res Opin.* 2016;32(1):133. doi: 10.1185/03007995.2015.1105795.
10. Pouresmaeili F., Kamalidehghan B., Kamarehei M., Goh Y.M. A comprehensive overview on osteoporosis and its risk factors. *Therapeutics and Clinical Risk Management.* 2018;14:2029-2049. doi: 10.2147/TCRM.S138000.
11. Liu W., Zhang X. Receptor activator of nuclear factor- κ B ligand (RANKL)/RANK/osteoprotegerin system in bone and other tissues (Review). *Molecular Medicine Reports.* 2015;11:3212-3218. doi: 10.3892/mmr.2015.3152.
12. Salamanna F., Borsari V., Brogini S. et al. A Human 3D In Vitro Model to Assess the Relationship Between Osteoporosis and Dissemination to Bone of Breast Cancer Tumor Cells. *J Cell Physiol.* 2017;232(7):1826-1834. doi: 10.1002/jcp.25708.
13. Buenostro D., Mulcrone P.L., Owens P., Sterling J.A. The Bone Microenvironment: a Fertile Soil for Tumor Growth. *Curr Osteoporosis Rep.* 2016;14(4):151. doi: 10.1007/s11914-016-0315-2.
14. Chen Z., Maricic M., Bassford T.L. et al. Fracture risk among breast cancer survivors: results from Women's Health Initiative Observational Study. *Arch Intern Med.* 2005;165(5):552.
15. Van Poznak C., Taxel P. Skeletal Complications of Breast and Prostate Cancer Therapies. *Primer on the Metabolic Bone Diseases and Disorders of Mineral Metabolism.* Eighth Edition. 2013, 719p.
16. Sturgeon K.M., Mathis K.M., Rogers C.J. et al. Cancer- and Chemotherapy-Induced Musculoskeletal Degradation. *JBM Plus.* 2019; 3(3):e10187. doi: 10.1002/jbm4.10187.
17. Bahney C.S., Zondervan R.L., Allison P. et al. Cellular biology of fracture healing. *Journal of Orthopaedic Research®.* 2019;37(1):35-50. doi: 10.1002/jor.24170.
18. Pountos I., Giannoudis P.V. Fracture Healing: Back to Basics and Latest Advances. *Fracture Reduction and Fixation Techniques.* 2018;3(17). doi: 10.1007/978-3-319-68628-8_1.
19. Choy M.H.V., Wong R.M.Y., Chow S.K.H. et al. How much do we know about the role of osteocytes in different phases of fracture healing? A systematic review. *Journal of orthopaedic translation.* 2020; 21:111-121. doi: 10.1016/j.jot.2019.07.005.
20. Straszkowski L., Jovic T., Castillo-Tandazo W. et al. Effects of chemotherapy agents used to treat pediatric acute lymphoblastic leukemia patients on bone parameters and longitudinal growth of juvenile mice. *Experimental Hematology.* 2020. doi:10.1016/j.exphem.2020.01.010.
21. Rana T., Chakrabarti A., Freeman M., Biswas S. Doxorubicin-mediated bone loss in breast cancer bone metastases is driven by an interplay between oxidative stress and induction of TGF β . *PLoS ONE.* 2013;8(11):e78043. doi: 10.1371/journal.pone.0078043.
22. Fonseca H. et al. Effects of doxorubicin administration on bone strength and quality in sedentary and physically active Wistar rats. *Osteoporosis International.* 2016;27(12):3465-3475. doi: 10.1007/s00198-016-3672-x.
23. Quach J.M., Askmyr M., Jovic T. et al. Myelosuppressive therapies significantly increase pro-inflammatory cytokines and directly cause bone loss. *Journal of Bone and Mineral Research.* 2015;30(5):886-897. doi: 10.1002/jbmr.2415-.
24. Fan C., Georgiou K.R., McKinnon R.A. et al. Combination chemotherapy with cyclophosphamide, epirubicin and 5-fluorouracil causes trabecular bone loss, bone marrow cell depletion and marrow adiposity in female rats. *J Bone Miner Metab.* 2016; 34:277-290. doi: 10.1007/s00774-015-0679-x.
25. Robin F., Cadiou S., Albert J.D. et al. Methotrexate osteopathy: five cases and systematic literature review. *Osteoporosis International.* 2020. doi: 10.1007/s00198-020-05664-x.
26. Georgiou K.R., King T.J., Scherer M.A. et al. Attenuated Wnt/ β -catenin signalling mediates methotrexate chemotherapy-induced bone loss and marrow adiposity in rats. *Bone.* 2012;50(6):1223-1233. doi: 10.1016/j.bone.2012.03.027.
27. Albers J., Keller J., Baranowsky A. et al. Canonical Wnt signaling inhibits osteoclastogenesis independent of osteoprotegerin. *The Journal of Cell Biology.* 2013;200(4):537-549. doi: 10.1083/jcb.201207142.
28. Olsen N.J., Spurlock C.F., Aune T.M. Methotrexate induces production of IL-1 and IL-6 in the monocytic cell line U937. *Arthritis research therapy.* 2014;16(1):1-8. doi: 10.1186/ar4444.

The study was performed within the planned research topic "Morphofunctional aspects of homeostasis", state registration number 0118U006611.

ORCID and contributionship:

Tetiana V. Riabenko: 0000-0003-2740-389X^D
 Alexey V. Korenkov: 0000-0002-1314-5642^F
 Serhii M. Dmytruk: 0000-0001-6434-2817^E
 Olha S. Yarmolenko: 0000-0002-7872-2308^A
 Alina A. Ponyrko: 0000-0002-1799-7789^B
 Mykolay S. Pernakov: 0000-0002-7048-7446^B
 Viktoriia I. Hula: 0000-0003-3869-5162^C

Conflict of interest:

The Authors declare no conflict of interest.

CORRESPONDING AUTHOR

Tetiana V. Riabenko
 Sumy State University
 31 Sanatorna st., 40018 Sumy, Ukraine
 tel: +380669362214
 e-mail: t.riabenko@med.sumdu.edu.ua

Received: 27.04.2021

Accepted: 28.11.2021

A – Work concept and design, **B** – Data collection and analysis, **C** – Responsibility for statistical analysis, **D** – Writing the article, **E** – Critical review, **F** – Final approval of the article